EPJ E
Soft Matter and Biological Physics
EPJ.org
your physics journal

Eur. Phys. J. E (2015) **38**: 124 DOI 10.1140/epje/i2015-15124-2

Segregation in a model system for tapped wet disks in two dimensions

Rodolfo O. Uñac, Luc Oger and Ana M. Vidales

edp sciences Società Italiana di Fisica Springer

Eur. Phys. J. E (2015) **38**: 124
DOI 10.1140/epje/i2015-15124-2

THE EUROPEAN PHYSICAL JOURNAL E

Regular Article

Segregation in a model system for tapped wet disks in two dimensions

Rodolfo O. Uñac[1], Luc Oger[2], and Ana M. Vidales[1,a]

[1] Departamento de Física, Instituto de Física Aplicada (UNSL-CONICET), Universidad Nacional de San Luis, Ejército de los Andes 950, D5700HHW San Luis, Argentina
[2] Institut de Physique de Rennes, UMR UR1-CNRS 6251, Université de Rennes1, 263, Avenue du General Leclerc, Campus de Beaulieu, CS 74205, 35042 Rennes Cedex, France

Received 8 June 2015 and Received in final form 26 August 2015
Published online: 30 November 2015 –

Abstract. The problem of segregation of mixtures in a column of wet disks subjected to tapping is studied through a simple model that simulates, through a pseudo-dynamics algorithm, the formation of the packing and the successive tapping of it. The particles consist in a binary mixture of disks with two different sizes and the capillary forces are simulated stochastically by a sticking probability between the particles. We have recently shown that arch formation is one of the chief mechanisms determining size segregation in a non-convecting ensemble of dry disks (R.O. Uñac *et al.*, Eur. Phys. J. E **37**, 117 (2014)). In the present paper, we focus on the special role that capillary bridges can have on this type of segregation process, besides the proven effect of the presence of arches. We find that humidity between grains can enhance the segregation process in a binary mixture. In particular, for the case of the segregation of an intruder, humidity can promote the rise of the big particle even in cases where the number or the size of the arches would not normally favor the climb.

1 Introduction

The problem of segregation of a granular medium is a longstanding one and has been studied deeply in the last decades given that it is present every time that grains with different properties are manipulated [1–5]. Both the type of action performed over the grains (vibration, pouring, shearing, etc.) and their properties (size, shape, density, roughness, among several others) are very often the causes of serious industrial problems where the separation of particles with different properties is undesirable [6–9].

Not all the mechanisms leading to segregation are yet well understood. In particular, size segregation by shaking or by tapping is still a matter of several questions [3,10–12]. The extent and possibilities for segregating a mixture of grains with different sizes will depend on the external excitation parameters like shaking intensity, frequency, external relative humidity, waiting time between perturbations, gravity, and so on. Besides, the properties of the sample are crucial, *i.e.*, the size ratio between particles, the size of the system, the presence of walls, the asymmetries in the response to excitations, the internal humidity and the presence of electrostatic interactions.

There are numerous models and numerical simulations of the above situations to study the influence of the various parameters, especially in the simple case of bidisperse grains with equal density and a smooth surface or, at least, where both species have the same roughness [13,14].

Despite the many parameters that come into play in the process of segregation, it is still surprising that the simple action of tapping a bidisperse sample of dry disks in a 2D container with a base and two vertical walls, and the mere presence of an asymmetry, like gravity, is enough to provoke size segregation. Even if this is a simple experiment, the relationship between arching and segregation has been demonstrated only recently. Indeed, there is a correlation between the number and size of the arches formed by a particle with its neighbours and its chance for rising in a column of smaller particles [15].

Although in real scenarios the presence of humidity is a questionless fact, considering capillary interactions between particles is not easy to model or measure when an experiment is performed. For that reason, much work still remains to be done in the field of wet granular matter. In the particular case of vibrated granular media, progress has been made in studying the influence of humidity on the segregation patterns [16,17]. However, there is still lacking, to our knowledge, of investigation on the effect that capillary bridges and arches can have in the chance for wet particles to segregate in a tapped column.

Given the interest of the topic and the results recently found for dry disks, we propose here studying the effect that humidity has in the segregation process that occurs

[a] e-mail: avidales@unsl.edu.ar

in bidisperse mixtures of wet disks in a vertical, rectangular container. To this end, we perform numerical simulations through a simple model that puts into relevance the geometric hindrance between particles, the asymmetry imposed by gravity and the changes in the interactions due to the presence of humidity between the grains. This last feature is simulated by a simple stochastic model.

2 Simulation model

2.1 Reference model

We base our study on simulations using a pseudo-dynamics algorithm that puts into interaction inelastic hard disks. This model has been designed by Manna and Khakhar [18] and has already been used previously by other authors [19,20] and in our own investigations [15,21, 22]. Unlike DEM simulations, the evaluation of the forces between particles (or any other dynamical interactions inside the system) is not performed. To govern the evolution of the system, we take into account the direction of gravity and the local geometrical constraints due to the presence of other grains. The disks are deposited in a 2D rectangular box. The pseudo-dynamics method consists in small falls and rolls of the grains until they come to rest by contacting other particles or the system boundaries. We use a container formed by a flat base and two flat vertical walls. No periodic boundary conditions are applied.

A particle in the container can have only two types of movements: it can either fall vertically along a length δ, or it can roll an arc-length δ over another particle in contact [19,20]. If, in the course of a fall of length δ, a disk collides with another disk (or the base), the falling disk is put just in contact and this contact is defined as its first supporting contact. Likewise, if during a roll a disk collides with another disk (or a wall), the rolling disk is put just in contact with this new one. If the first supporting contact and the new contact are such that the disk is in a stable position (the horizontal coordinate of the center of the disk falls in between the ones of the two contacts), the second contact is defined as the second supporting contact; otherwise, the lower of the two contacting particles is taken as the first supporting contact of the rolling disk and the second supporting contact is left undefined. If, during a roll, a particle reaches the same height as the supporting particle, this first supporting contact is left undefined (in this way the particle will fall vertically in the next step instead of rolling underneath the first contact). Disks with two supporting contacts are considered stable and left in their positions.

A moving disk can change the stability state of other disks supported by it, therefore, this information is updated after each move. The full process of deposition is over once each particle in the system has two supporting contacts defined or is in contact with the base (particles at the base are supported by a single contact). The coordinates of the centers of the disks and the corresponding labels of the two supporting particles, wall, or base, are saved for analysis.

For very small values of δ, this method yields a realistic simultaneous deposition of grains with zero restitution coefficient. We chose $\delta = 0.0124r$ (with r the radius of the smaller particle in the system) since results for smaller values of δ show to be indistinguishable from those presented here [20]. Simulations are carried out in a rectangular box of width $49.56r$ containing 1500 disks of two different radii r and R, where R is the radius of the big particles. This number of particles is large enough to avoid scaling effects and it is small enough to make tractable the simulation time in a large tapping process like the one implemented here.

As we will see below, two kinds of situations are studied here to analyze the effect that humidity has on a segregation process by tapping. First, the segregation under tapping of a single large particle of radius R (the intruder) surrounded by smaller particles of radius r is studied. It is known that for such system in dry conditions, the intruder may raise to the top of the column or not, depending on the size ratio R/r and vibration intensity [23,15]. We want to prove here how humidity can affect the critical size ratio for the segregation of the intruder with the same tapping amplitude.

Secondly, the segregation of binary mixtures with a given size ratio R/r is studied. The concentration of big particles is defined through the value of X as the ratio of area occupied by big and small disks, *i.e.*, $X = (N_\mathrm{b}/N_\mathrm{s})(R/r)^2$, where N_b is the number of big disks and N_s the corresponding to small ones. The results presented below correspond to $X = 0.25$ and $R/r = 3.0$, but other concentrations (where X is always less than 1) have been inspected. The results are not substantially different than the ones presented in the next sections.

2.2 Simulation of the cohesion forces

When humidity is present between the grains of a granular packing, the extent of the changes in its behavior will depend, as could be expected, on the amount of liquid distributed between the grains. Thus, several states can be distinguished for a granular ensemble as a function of humidity content [24].

In particular, a wet granular sample at low liquid content presents a network of capillary bridges connecting the grains and this network will be crucial in determining the segregation behavior of the system [16]. In the present study, we consider situations where cohesion predominates over other effects of the presence of liquid in the system such as lubrication and viscosity [17]. Our model represents a granular assembly in the so called "pendular state" according to the classification by liquid content [24]. In the pendular state, particles are held together by the attraction of the capillary bridges at their contact points.

As the result of a non-equilibrium thermodynamic situation, a capillary bridge is formed thanks to the collapse of the liquid film that covers the surface of two grains, thus bending with a given curvature and forming the mentioned bridge [25]. If the particles are moved away from each

other by a certain distance, a so-called pendular bridge appears due to the bridge stretching [26].

Among the different factors affecting the total capillary force in a static liquid bridge [27], we consider here that the contact angle is zero (complete wet) and that the surface tension of the liquid is constant all over the system. Other variables as the separation distance between the two particles participating in the formation of the liquid bridge and the volume of the liquid bridge, are considered here as stochastic variables since each bridge in the system may have a different volume and separation depending on local conditions and contact history. Moreover, in a real scenario, the liquid is not necessarily uniformly distributed over the disks, and the formation of a liquid bridge also depends on the rugosity of the particle surface [26]. In our model, the choice of a sticking probability somehow simulates these variables that are otherwise difficult to characterize. These important factors are introduced in the simulations through a single parameter P_0 which is described below. Besides, in our model, we only count as a capillary bridge, the contact between two particles that is able, alone, to fully stabilize one of the touching grains.

It is important to notice that, in a real pendular state, some capillary bridges formed between particles do not necessarily contribute to the stabilization of the particles. This situation is not taken into account in our present simulations.

In fig. 1 we show the force balance situation of two disks in contact. A given particle i, with a driving force due to gravity W, is in contact with a lower partner j. We define γ as the angle formed by the segment joining the two centers of the two particles in contact and the horizontal (see fig. 1). Assuming that the suction $F_{\rm suc}$ [17] does not depend on the angle γ, the forces involved will be

$$\mathbf{F}_{\rm n} = \mathbf{F}_{\rm suc} + \mathbf{W}_{\rm n} = (F_{\rm suc} + W\sin(\gamma))\hat{\mathbf{n}} \quad \text{in the normal direction of the contact,} \tag{1}$$

$$\mathbf{F}_{\rm t} = W\cos(\gamma)\hat{\mathbf{t}} \quad \text{in the tangential direction.} \tag{2}$$

Provided that particle j is fixed in its position, the normal force $\mathbf{F}_{\rm n}$ is responsible for the adhesion of particle i onto the bottom partner j. Further, the tangential force $\mathbf{F}_{\rm t}$ provides the torque that drives particle i into rolling on top of particle j. Let us assume that the average suction is x times the driving force due to gravity for a small particle (*i.e.*, $F_{\rm suc} = xW^{\rm s}$), where $W^{\rm s}$ is the driving force for the small particle. We consider bidisperse systems where the particles have two different driving forces. Then, we have, for small (or big) particles, $F_{\rm n}^{\rm s(b)} = W^{\rm s}[x + (\frac{W^{\rm s(b)}}{W^{\rm s}})\sin(\gamma)]$. This means that the total forces that are responsible for maintaining the particles (small or big) in contact with any particle will vary between $W^{\rm s(b)}[x + (\frac{W^{\rm s(b)}}{W^{\rm s}})]$ and $W^{\rm s(b)}[x - (\frac{W^{\rm s(b)}}{W^{\rm s}})]$ for a small or a big particle rolling over any other particle as γ goes from $\pi/2$ to $-\pi/2$. For $x < 1$, negative values of $F_{\rm n}$ are obtained for some configurations of dangling disks. This corresponds to the normal component of the particle driving force overcoming the suction, which invariably leads to the detachment of the dangling disk.

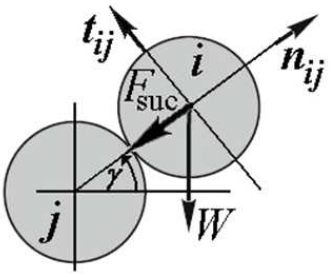

Fig. 1. Schematic diagram of the forces acting on a particle i which is forming a capillary bridge after contacting another particle j during deposition.

In our model, we implement capillary bridges through a stochastic mechanism so that a particle may be stuck during its rolling down over another particle due to suction. The actual sticky probability $P_{\rm sticky}^{\rm s(b)}$ is then proportional to the normal force applied on the rolling particle at a given angle γ measured from the horizontal [22]. Thus, it is given by

$$P_{\rm sticky}^{\rm s(b)}(\gamma) = \max\left\{0, P_0\frac{\left[x + \left(\frac{W^{\rm s(b)}}{W^{\rm s}}\right)\sin(\gamma)\right]}{x+1}\right\}. \tag{3}$$

In eq. (3) we have divided the normal force by its maximum possible value and introduced the proportionality constant P_0 to control the maximum sticky probability: $P_0 = 1$ means that stickiness is maximum whereas $P_0 = 0$ means that particles do not stick (dry case). Through this simple modelization, we are able to study different "wetting" conditions between particles, thus emulating different degrees of humidity in the pendular state. Moreover, as we assume that all particles have the same density and our system is two-dimensional, we can replace $\frac{W^{\rm s(b)}}{W^{\rm s}}$ by $(\frac{R}{r})^2$. It is important to say that, in our model, the increment of the volume of water present in each bridge is not defined and only the existence or not of a liquid bond is considered. Thus, any discussion about the total humidity present in the system is not possible to develop. For that reason, the link to the wetting status of the column is made through P_0.

The max function in eq. (3) takes care of the situation where $x < 1$ for which the second argument may become negative indicating that the particle must detach (*i.e.*, $P_{\rm sticky}^{\rm s(b)}(\gamma) = 0$). Nevertheless, all our simulations have been carried out setting $x = 1$.

2.3 Packings of sticky disks

The pseudo-dynamics of the sticky disks follows the same rules as explained elsewhere [21,22], and it is mainly the same as for dry hard disks. In this section we will provide a guide explanation just recalling some of its main aspects and suggest to the reader to go to [21] for deeper details.

If in a given iteration a disk already has one single potential supporting contact there are two possibilities: i) to stick through a capillary bridge to the supporting particle and so become immobilized (probability $P^{\mathrm{s(b)}}_{\mathrm{sticky}}(\gamma)$), or ii) to move on by either a roll or a free fall. A particle that sticks is an example of the situation in which the strength of the capillary bridge is enough to prevent the particle from further rolling on top of its supporting disk. If the supporting particle does not move further in future time steps the disk will remain in its stable position held by the capillary bridge.

A particle that does not stick to its first potential support (probability $[1 - P^{\mathrm{s(b)}}_{\mathrm{sticky}}(\gamma)]$) corresponds to the situation in which either a capillary bridge does not form at the contact or the driving force of the disk overcomes the strength of the capillary bridge. For this reason the particle can roll down the surface of the lower partner. If a bridge exists, and the suction is not too weak, one expects that the particle may keep rolling without detaching from the surface of the contacting disk even after reaching a lower position with respect to its partner. All along the rolling, the disk has a chance to stick $[P^{\mathrm{s(b)}}_{\mathrm{sticky}}(\gamma)]$ at every iteration and become immobilized. At each step, the chance is independent of the previous iteration. However, once the particle has rolled to a position beneath its supporting partner, and provided that the particle does not stick, there is a probability for the particle to detach and fall freely, and a probability for it to keep rolling in contact. We use again $[P^{\mathrm{s(b)}}_{\mathrm{sticky}}(\gamma)]$ to set the probability that a particle dangling beneath its support will roll in contact without detaching [21]. This probability does not need to be the same as the sticky probability, but it has to be related to the strength of the capillary bridge. We have chosen $[P^{\mathrm{s(b)}}_{\mathrm{sticky}}(\gamma)]$ for this probability in order to reduce the number of control parameters in the model. Notice that in this case the disk is not stuck—*i.e.*, it is not immobilized—but remains in contact. In the next iteration, the disk will again have the chance to stick. It is worth mentioning that, since in our simulations $P^{\mathrm{s}}_{\mathrm{sticky}}(-\frac{\pi}{2}) = P^{\mathrm{b}}_{\mathrm{sticky}}(-\gamma_{\mathrm{c}}) = 0$ (recall that $x = 1$), where $\gamma_{\mathrm{c}} = \sin^{-1}[(\frac{r}{R})^2]$, all particles that do not stick but roll dangling from its partner will eventually detach at the point $\gamma = -\frac{\pi}{2}$ for small particles and $\gamma = -\gamma_{\mathrm{c}}$ for big ones, unless a second contact is formed during rolling.

In summary, a particle that contacts another disk with $0 < \gamma < \pi/2$ has a probability $P^{\mathrm{s(b)}}_{\mathrm{sticky}}(\gamma)$ to stick and a probability $[1-P^{\mathrm{s(b)}}_{\mathrm{sticky}}(\gamma)]$ to roll. However, if $(-\pi/2 < \gamma < 0)$ for a small particle, or $(-\gamma_{\mathrm{c}} < \gamma < 0)$ for the bigger, the particle has a probability $P^{\mathrm{s(b)}}_{\mathrm{sticky}}(\gamma)$ to stick, a probability $[1 - P^{\mathrm{s(b)}}_{\mathrm{sticky}}(\gamma)][P^{\mathrm{s(b)}}_{\mathrm{sticky}}(\gamma)]$ to roll, and a probability $[(1 - P^{\mathrm{s(b)}}_{\mathrm{sticky}}(\gamma))^2]$ to detach.

2.4 Tapping process on the columns

Initially, the configuration is obtained by placing the disks at random in the space inside the simulation box, with a very low packing fraction. An initial deposition takes the system to its first stable configuration. After the array of particles attains a stable configuration, a tapping process is started. All vertical coordinates of the particles are multiplied by a factor $A > 1$. The disks are also subjected to Monte Carlo steps (around 20) to randomly move small displacements, ξ, in both directions, horizontal and vertical, uniformly distributed in the length range $0 < \xi < A - 1$ [21]. New configurations having overlapped disks are rejected. This disordering stage is important to avoid particles falling back again into the same positions. Moreover, the upper limit for the random displacements (*i.e.* $A - 1$) is deliberately chosen so that a larger tap promotes larger random changes in the particle positions.

It should be noted that, before a tap, all particles are effectively disconnected, with no contacts between them. Besides, for $P_0 \neq 0$, all the liquid bridges are removed, thereby preventing the formation of permanent clusters. This of course will avoid the possible correlations that clumps formed in a previous deposition could introduce to the structure of the packing.

The tapping intensity A ranges from 1.1 to 2.0. For each value of A and each size ratio R/r studied, 5×10^3 taps are applied to the sample.

The Manna *et al.* method [18] has the advantage that fully static configurations are obtained after each tap with each disk sustained by other two disks by definition, in the dry case. All the history of formation of the packing can be followed during the simulation. This leads to a straightforward definition of the arches in the system and the knowledge of the capillary bridges between particles. This can be also done, although with much more computational effort, on molecular dynamic type simulations [28].

2.5 Identification of arches and capillary bridges

As said before, the role of arches in the segregation of a column of particles of different sizes is one of the key points to understand the problem [15,23,29,30]. As we will see in this paper, the behavior of arches in the presence of humidity is crucial in the explanation of the values of the segregation indices for mixtures at a given humidity content represented by P_0.

Arches can be readily extracted from our pseudo-dynamics simulations since they are defined by construction of the granular sample and we know all the formation history of the packing [15].

Two disks A and B are said mutually stable if A is the left supporting particle of B and B is the right supporting particle of A, or vice versa. Arches are sets of mutually stabilizing particles in a static granular sample [31,32]. In our pseudo-dynamics simulations we first identify all mutually stable particles and then find the arches as chains of particles connected through these mutual stability contacts. Since our algorithm rests on defining which disk is a support for another disk during the deposition, this information is available in our simulations.

Details on the properties of arches found in pseudo-dynamics simulations can be found in previous

works [15,20,33,21]. One interesting feature to remark is that arches are much less preeminent in regions where ordering is present [15]. In particular, for monosized systems at different tap intensities where an order-disorder transition is observed, there is a sudden drop in number of arches in the ordered phase [33].

One of our objectives in this work is to put into evidence the role that humidity has on the segregation process in the case of an ascending intruder. In this case, the behavior of the capillary bridges as a function of tapping number and P_0 is important to explain the differences in the critical size ratios for ascension of a dry intruder compared to that for a wet one. The determination of this number is straightforward in our simulations. Each time a particle sticks to another, forming thus a capillary bridge, we label that contact and keep the label as soon as the bridge is conserved following the rules explained in sect. 2.3. When the column of disks has attained a stable configuration, we can easily count the labels and determine the number of bridges present in those configurations.

3 Results and discussion

3.1 Segregation for a wet intruder

As said before, one of our interests consists in studying the behavior of an intruder, *i.e.*, a single big particle with radius R, submerged in a bath of 1499 smaller particles of radius r, all of them contained in a rectangular box, as described in a previous section, and subjected to a tapping process.

The first important result is that the critical size at which an intruder is able to reach the top of the column is notably changed under the presence of humidity. In fig. 2(a) we show the height of the intruder (initially placed at the bottom of the simulation box) as a function of the number of taps applied to the system with $A = 1.1$ and $P_0 = 0.01$. At these low tap intensities, the wet intruder still rises to the top of the column even for $R/r = 4.0$. Surprisingly, this ratio is less than the one expected for a dry intruder, which was 4.5. Even more, for $R/r = 3.0$, the wet intruder reaches higher inside the column than does the dry one, although neither of them succeed in reach the top for the tapping numbers investigated [15]. For ratios less than 3.0, the intruder practically remains at the bottom of the system and, eventually, only rises up a few small particle diameters, like in a dry system.

Figure 2(b) shows the case for $A = 1.1$ and $P_0 = 0.10$ where even an intruder with a ratio $R/r = 2.5$ almost reaches the top of the column. Note that the top most of the column (*i.e.*, the maximum height of the packing) is higher in this case than for the previous humidity value, in agreement with a looser structure caused by a larger number of capillary bridges [21]. In simulations and experiments [29,34–36], the reference to a transition between one state with a trapped intruder to one with an intruder that reaches the top, is often used and a critical size ratio is sought for each case. In our present results and in the context of our model, one can state that capillary bridges produce a shift down for the critical ratio.

The second result is that an increase in the tapping intensity enhances both the probability of the intruder to reach the surface and the rise velocity, even for small size ratios. This is shown in fig. 2(c). For $R/r = 2.0$, a small oscillation is observed after the intruder completely rises and for $R/r = 1.5$, the intruder sinks in the bulk after reaching the top and it is not clear if, in a longer tapping process, it would eventually rise again. It is important to remark that the top most height of the tapped column also increases with tapping intensity [21].

For higher humidity, the intruders of all size ratios inspected succeed in reaching the surface, as shown in fig. 2(d). A singular behavior is found in the present scenario. First, for the larger size ratio, the behavior is similar to the preceding case, *i.e.*, once the big particle rises to the surface, it stays on it. For intermediate size ratios, the intruder gets to the top, then gradually sinks into the bulk, and it never emerges again. Finally, for the smaller size ratios studied, the intruder presents oscillations of great amplitude between the top and the bulk of the column. These oscillations are not due to convection rolls because, as explained in earlier papers, they are not present in these simulations [15]. They are rather due to the competition between the intruder size ratio (to a larger size, a higher rising probability) and the probability of occurrence of the capillary bridges, which depends on the particle size (to a smaller particle size, a higher probability for the creation of a capillary bridge). In fig. 3 we show a snapshot of the trajectory of the oscillating intruder for $A = 1.3$, $P_0 = 0.10$ and $R/r = 1.5$.

Figure 4 shows the mean velocity of the intruders (in arbitrary units) with different ratios for $A = 1.10$ and three different humidity contents. This velocity is calculated as the mean slope in the corresponding plots of the height of the intruder *vs.* tapping number. The effect of humidity is clear. For the dry case there is a net transition at $R/r = 4.5$ [15]. For low humidity, the transition shifts around $R/r = 2.5$ to 3.0, while for a higher humidity, it disappears. On the other hand, at a given size ratio, the rising velocity is larger for larger humidity content. Notice however that these values will depend on the vibration intensity.

Another important finding is the role of both, arches and capillary bridges, in the climbing of the intruders.

As humidity increases, the average size of the arches where the big particle is participating is smaller during all the tapping process (fig. 5(a)). Nevertheless, the mean size of those arches is enough for the big particle to rise. This is in agreement with the behavior of the percentage of configurations without arches (fig. 5(b)), which is low up to 1000 tappings. As expected, once the intruder gets to the surface of the packing, the mean size of the arches becomes smaller (tending to zero) and, as a consequence, the percentage in fig. 5(b) tends to 100%. This puts into evidence the role of arches in the climb for the large size ratio 5.0. Besides, it is important to notice that the increase in the number of capillary bridges enhances the rise of the intruder, as can be appreciated in fig. 5.

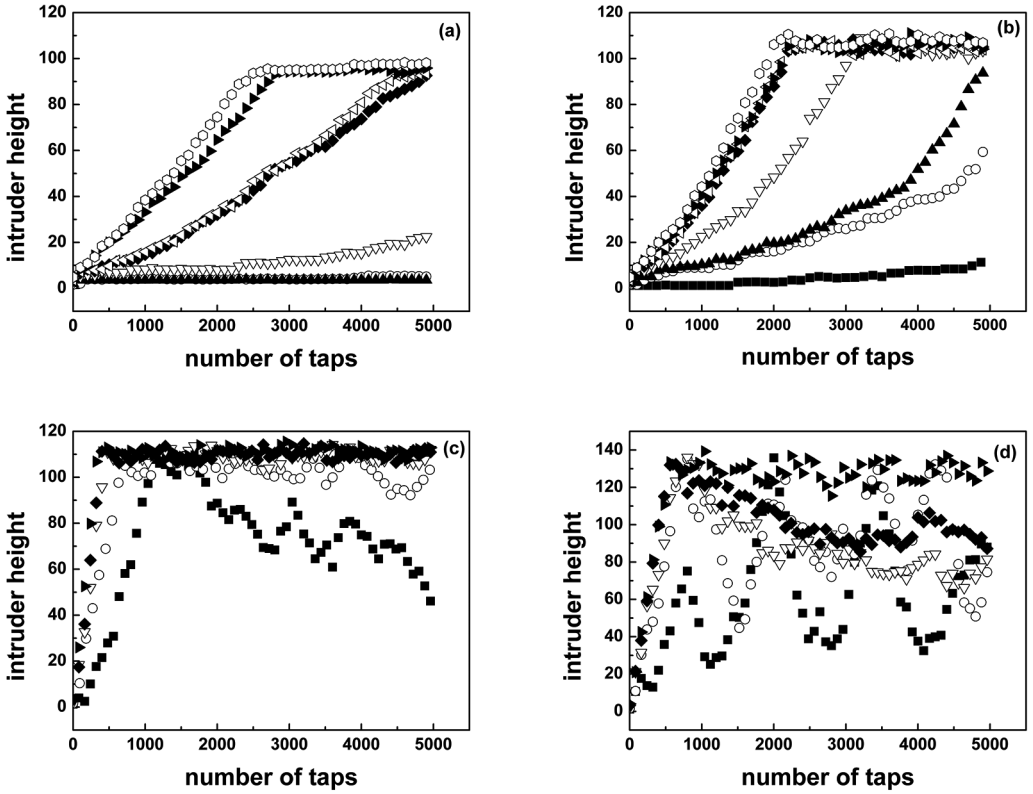

Fig. 2. Height of the intruder (in arbitrary units) as a function of the number of taps applied to the system for (a) $A = 1.1$ and $P_0 = 0.01$; (b) $A = 1.1$ and $P_0 = 0.1$; (c) $A = 1.3$ and $P_0 = 0.01$; and (d) $A = 1.3$ and $P_0 = 0.10$. The size ratios, R/r, are represented as: solid squares, 1.5; open circles, 2.0; solid up triangles, 2.5; open down triangles, 3.0; solid diamonds, 4.0; open left triangle, 4.5; solid right triangle, 5.0 and open hexagon, 6.0.

The behavior for $R/r = 3.0$ has some differences (fig. 6). On the one hand, a reduction in the mean size of the arches is also observed as humidity increases and, as in the dry case, the size is, in average, smaller than for $R/r = 5.0$ [15]. On the other hand, and even having a larger mean size for arches in the case of $P_0 = 0.01$ than for $P_0 = 0.1$, it is important to remember (fig. 2(a)) that the intruder for $R/r = 3.0$ does not get to the top of the column for $P_0 = 0.01$, while for $P_0 = 0.1$ it does segregate. Here, the role of capillary bridges becomes even more important, as we will see below.

The percentage of configurations without arch is especially high for $P_0 = 0.1$, while for $P_0 = 0.01$ it is more comparable to the dry case. This would lead to expect that the intruder will be unable to reach the top of the column. Nevertheless, as already demonstrated above, for a high humidity value, the intruder succeeds to segregate.

Finally, in fig. 7(a) and (b), we show the average number of capillary bridges per particle, in the whole system, for $P_0 = 0.01$ and $P_0 = 0.1$, respectively. In parts (c) and (d) of the same figure, we plot the average number of capillary bridges formed by the intruder. All columns are tapped at $A = 1.1$. It is important to say that capillary bridges have their own history of formation. They occur during the pseudo-dynamical relaxation process, with a given probability, when two particles are in contact. Besides, that two particles are in contact, is the result of the present configuration, which, in turn, is correlated to the previous history of the packing.

The average number of bridges for all the particles at low humidity has a mild decrease as the tapping proceeds (fig. 7(a)), and it is very similar for both size ratios. For $R/r = 3.0$, the decrease is greater at the first two hundred taps and practically stays unchanged for the rest of the simulation. For $R/r = 5.0$, the drop is smoother and sustained over all the tapping process. Nevertheless, one may say that both systems present similar features regarding the total number of capillary bridges and that the size of either intruder does not affect greatly the global behavior. The same conclusion could be drawn for the behavior at $P_0 = 0.1$ (fig. 7(b)), although the average number of bridges is markedly higher.

The behavior of the number of capillary bridges that support the intruder at low humidity is different for different size ratios. In average, the smaller intruder forms less supporting bridges with the bath of particles than the bigger one (see fig. 7(c)). This lower number, and the fact that arches are smaller for $R/r = 3.0$ compared to $R/r = 5.0$ (see part (a) in figs. 5 and 6), does not make the intruder to ascend. For $P_0 = 0.1$, the number of capillary bridges for the intruder drastically increases for both size ratios, as seen in fig. 7(d). Here the smaller intruder

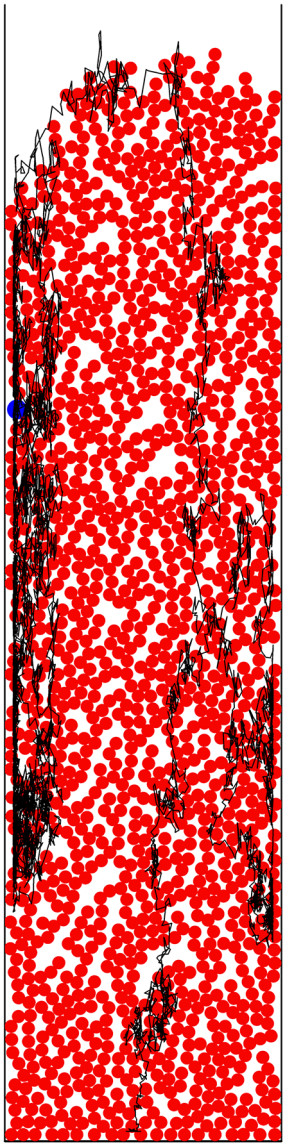

Fig. 3. Trajectory of an intruder for $A = 1.3$, $P_0 = 0.10$ and $R/r = 1.5$. The intruder is initially placed at the bottom of the column. This snapshot can be compared with fig. 2(d), where one of the curves corresponds to this case. The configuration of the disks corresponds to their stable position after the last tap.

forms, in average, the same number of bridges as the bigger intruder does in the course of the tapping process. Thus, the smaller particle has a better chance to rise.

3.2 Segregation in a wet mixture

As in the case of dry binary mixtures previously studied [15], we work here with the size ratio $R/r = 3.0$, with a total of 1500 disks and a concentration $X = 0.25$, *i.e.*, $N_b = 40$ and $N_s = 1460$. We also examine other size ratios and concentrations, but the results are qualitatively the same as the ones presented below. For instance, in the

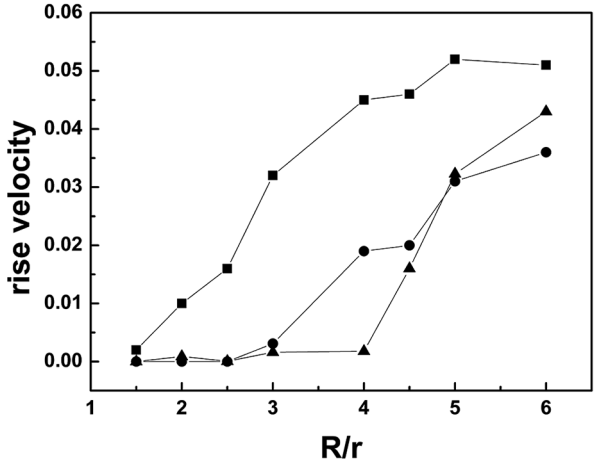

Fig. 4. Mean velocity of the intruders (in arbitrary units) for different size ratios and for $A = 1.10$ and three different humidity contents: $P_0 = 0.00$ (triangles), $P_0 = 0.01$ (circles) and $P_0 = 0.10$ (squares).

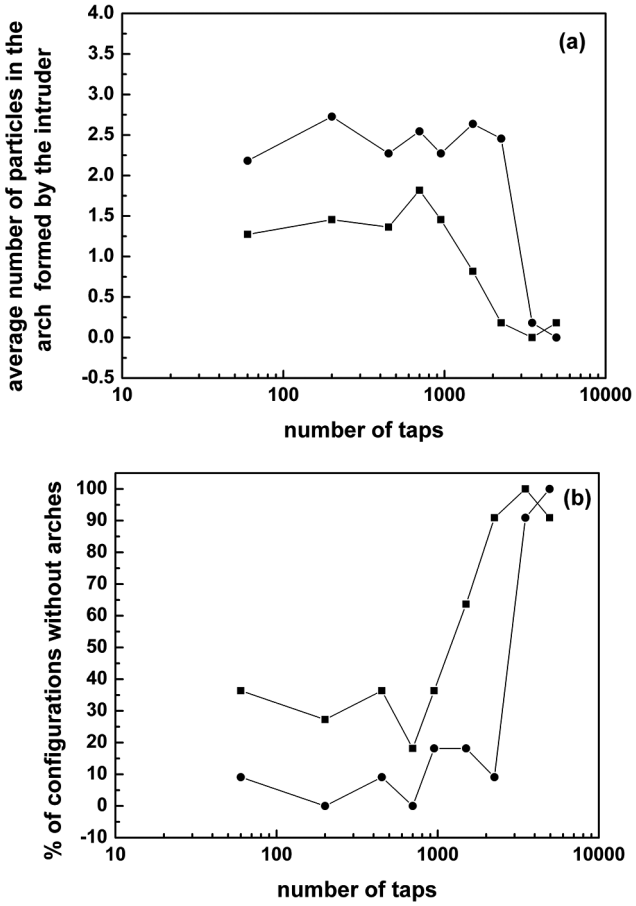

Fig. 5. (a) Average number of particles participating in the arch formed by the intruder as a function of the number of taps for $A = 1.1$ and $R/r = 5.0$, $P_0 = 0.01$ (circles) and $P_0 = 0.1$ (squares). (b) Percentage of configurations where the intruder does not form any arch as a function of the number of taps for $A = 1.1$ and $R/r = 5.0$, $P_0 = 0.01$ (circles) and $P_0 = 0.1$ (squares). The size of the arch is averaged over a dozen configurations taken every ten taps at chosen intervals along the process.

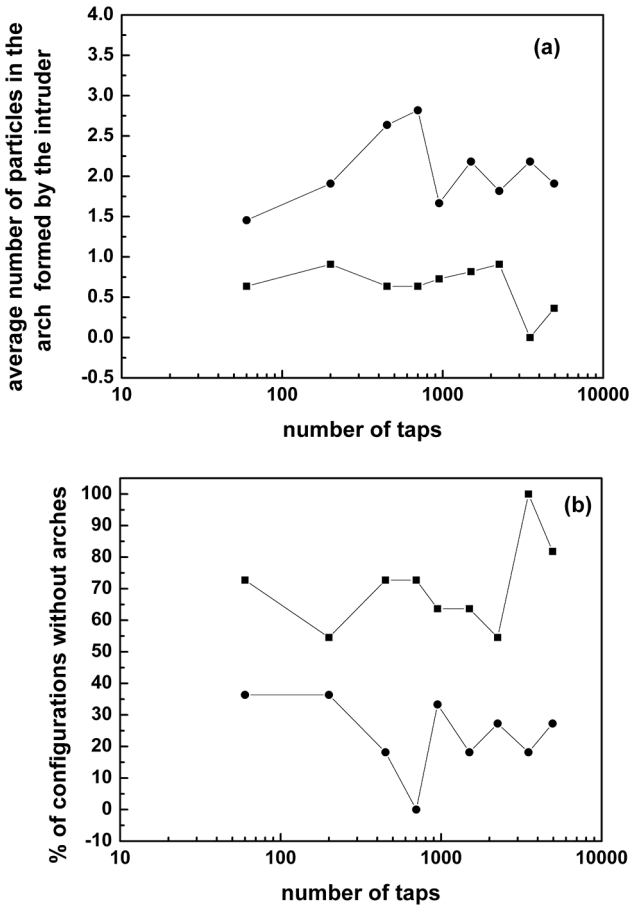

Fig. 6. (a) Average number of particles participating in the arch formed by the intruder as a function of the number of taps for $A = 1.1$ and $R/r = 3.0$, $P_0 = 0.01$ (circles) and $P_0 = 0.1$ (squares). (b) Percentage of configurations where the intruder does not form any arch as a function of the number of taps for $A = 1.1$ and $R/r = 3.0$, $P_0 = 0.01$ (circles) and $P_0 = 0.1$ (squares). The size of the arch is averaged over a dozen configurations taken every ten taps at chosen intervals along the process.

case of $X = 0.5$ or $X = 0.75$, for the same $R/r = 3.0$, the results do not change considerably because the introduction of more big particles in the mixture does not accelerate the segregation process. In the case of other size ratios, we have just preliminary inspected size ratios close to 3.0 (between $R/r = 3.0$ up to 3.5) and we did not found any substantial difference. We study three different sticking probabilities with $P_0 = 0.01$, 0.10 and 0.25. The results for this last humidity value are qualitatively similar to those for $P_0 = 0.10$.

After each tap, we analyze the resulting stable configuration. Two different indices are used to characterize the segregation process as a function of the number of taps. The first index is defined as

$$I_1 = 2\frac{H_\mathrm{s} - H_\mathrm{b}}{H_\mathrm{s} + H_\mathrm{b}} \tag{4}$$

Cimarra *et al.* [4] defined the same index, where H_s and H_b are the mean height for small and big particles, respectively. I_1 is zero if the system is well mixed in the vertical direction and, when big particles tend to segregate to the top of the column during tapping, I_1 becomes negative. Its minimum value will depend on the particular parameters of the mixture, *i.e.*, size ratio and concentration X of disks.

To show the evolution of the contacts between particles of different sizes, we define a second index I_2 that counts the number of contacts N_sb between disks of different radius. Thus, dividing this number by the total number of particles, N, we obtain the second index as: $I_2 = N_\mathrm{sb}/N$. It is expected that, as the segregation proceeds, I_2 will attain smaller values. When the phases of big and small particles completely separate, I_2 fluctuates around the fraction number of contacts at the interface between the two phases, *i.e.*, the upper phase of big particles and the bottom phase of small particles.

Results below show that the increase in the tapping intensity contributes to enhance the segregation velocity and, at high humidity, that capillary bridges build a looser structure, giving a higher segregation degree.

Figure 8 shows the evolution of I_1 as a function of the tapping number until 5000 taps. We compare the results for different levels of humidity with the dry case and for different A. Concerning the influence of the tapping intensity in both wet and dry cases, it is observed that an increase in A contributes to an increment in the segregation velocity. For $A = 1.1$, we observe a different behavior for $P_0 = 0$ and $P_0 = 0.01$ (fig. 8(a) and (b)) compared with $P_0 = 0.1$ (fig. 8(c)). At low humidity, the column does not segregate completely even up to 5000 tappings. However, for high humidity, the system reaches a totally segregated state. This is because, at a low amplitude and low humidity, the grains significantly compact, favoring the entrapment of the larger particles [15]. On the other hand, for greater humidity, the presence of capillary bridges causes a more loose structure, producing a higher segregation degree.

Figure 8(d) compares the segregation process for $A = 1.1$ and the three different humidity degrees chosen for simulations. The delay in the segregation process for the wet cases is clear compared with the dry case. Nevertheless, around tapping 2000, a change in the velocity of the process is observed and the wet cases segregate more quickly than the dry one. The increase in compaction with the number of tappings in the dry and low humidity cases, as already reported in [21], could explain the crossing of the curves in fig. 8(d), along with the behavior observed for arches as humidity increases, as we will see below.

A similar analysis can be performed for the other tapping intensities. At a given A, the segregation process is slower as humidity is higher. The explanation of this behavior is based on the analysis of the arches as the tapping intensity and humidity increase, as we will show below.

It is worthy to say that the behavior for higher humidities is quite similar to the one found for 0.1 and does not provide many more elements to the discussion.

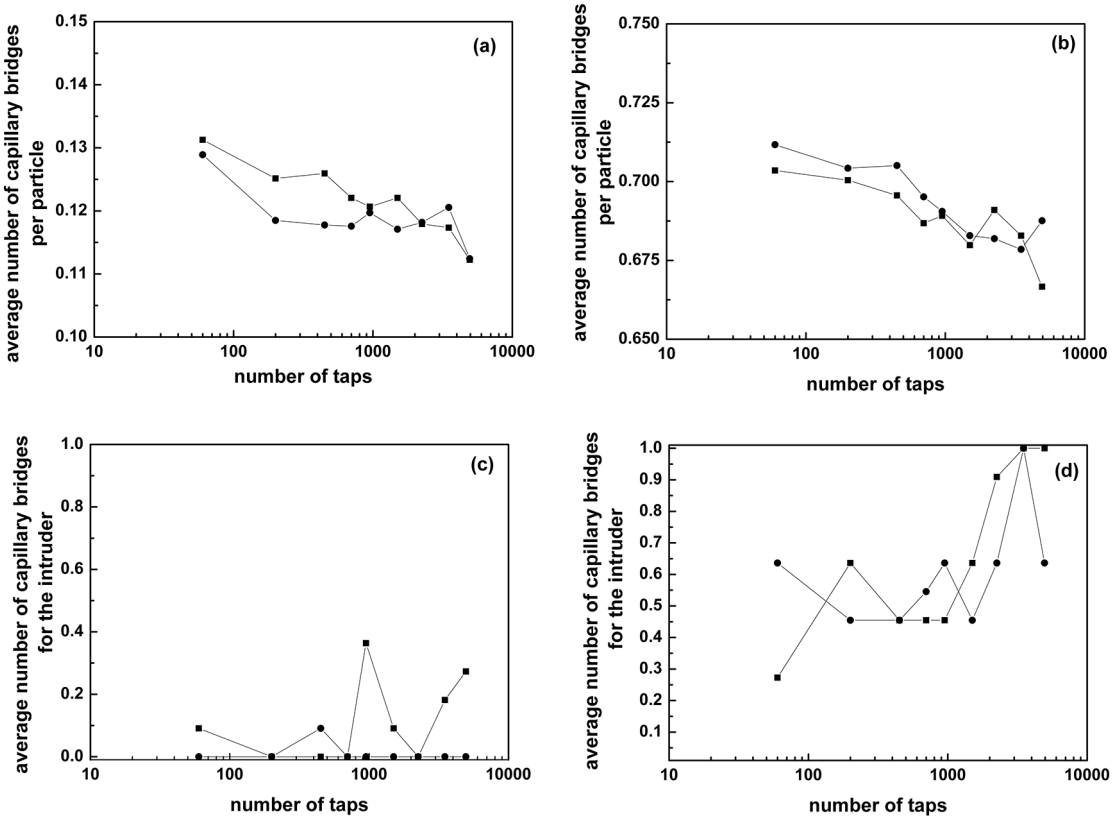

Fig. 7. Results for $A = 1.1$, $R/r = 3.0$ (circles) and $R/r = 5.0$ (squares). Average number of capillary bridges per particle, for all the particles in the system *vs.* the number of tappings: (a) $P_0 = 0.01$; (b) $P_0 = 0.1$. Average number of capillary bridges supporting the intruder *vs.* the number of tappings: (c) $P_0 = 0.01$; (d) $P_0 = 0.1$. The number of bridges is averaged over a dozen configurations taken every ten taps at chosen intervals along the process.

In fig. 9 we present the results for segregation index I_2. As in the case of dry columns [15], I_2 presents larger fluctuations than I_1 all over the segregation process. While I_1 decays slightly initially, the contacts between disks of different sizes —characterized by I_2— do not change significantly during the first 50 tap for the dry case, even at large tap intensities. This effect extends even more as humidity increases. This is due to the fact that, although large disks move upwards as soon as tapping begins — making I_1 decrease— they all remain surrounded by small disks during the initial stages of the segregation process. I_1 captures any large scale vertical segregation, while I_2 only features local segregation (such as cluster formation or domain growth, also those induced by capillary bridges). The results shown in fig. 9 indicate that segregation by clustering is not present in our simulations even in wet columns; only the formation of a domain of large disks at the top of the system drives the decrease of I_2. This feature may be related to the fact that we break the capillary bridges each time a new upward expansion begins.

The behavior of I_1 and I_2 for a greater concentration of large disks (always $X < 1$) is rather similar to the one shown in fig. 9.

The following results explain the role of arches and humidity in the way that segregation develops in the tapped columns.

Figures 10(a) and 11(a) show the evolution of the fraction of large particles not belonging to arches as tapping proceeds, for two different humidity contents, different amplitudes and $R/r = 3.0$. Despite the humidity content, the fraction increases with the tapping number. Besides, during the first series of taps, this fraction rises with humidity and, for a given P_0, it also increases as the tapping intensity is larger. The slopes of the different curves are milder as humidity is higher. We recall that for the dry case, the increment of the fraction is steeper than for the wet one (see [15] for details). Similarly, the fraction of particles belonging to arches with at least one large particle (fig. 10(b) and 11(b)) is, on average, lower for higher humidity and higher A, while, as the number of taps increases, decreases smoothly. For the dry case, the fraction drops rapidly from the first 100 taps. This behavior, together with the corresponding one shown in figs. 10(a) and 11(a), justifies the crossing of the segregation indices I_1, around 2000 taps, for $A = 1.1$ (fig. 8(d)).

Figure 12 presents the fraction of particles involved in arches (regardless of the size of the disks). The first to be said is that the average number of total particles belonging to arches decreases for greater values of A and, in turn, with humidity degree. It is important to note the scale used in fig. 12(b). The behavior found for $P_0 = 0.01$ and $A = 1.1$ is close to the one corresponding to the dry case,

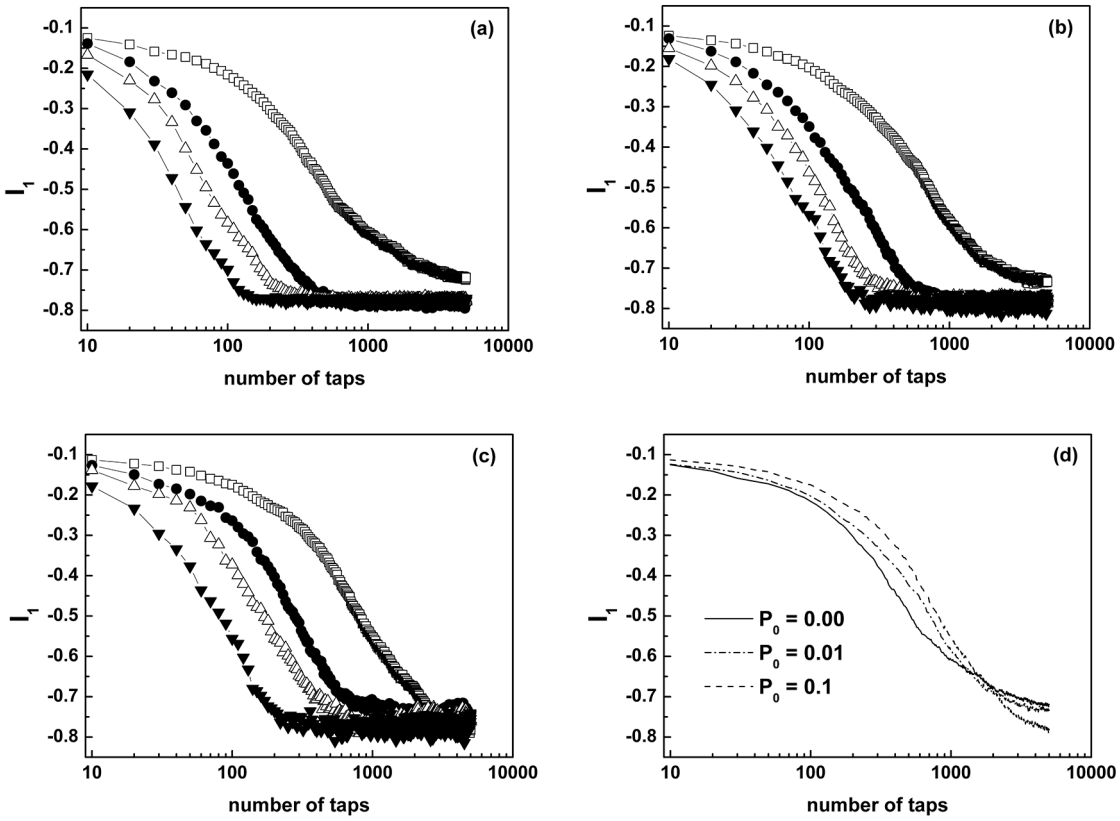

Fig. 8. Segregation index I_1 *vs.* tapping number. (a) $P_0 = 0.00$, (b) $P_0 = 0.01$, (c) $P_0 = 0.10$. In the three plots (a), (b), (c), A is represented by squares, 1.1; solid circles, 1.3; up triangles, 1.5; and solid down triangles, 2.0. (d) Comparison of I_1 when $A = 1.1$ and the three different humidity degrees chosen for simulations.

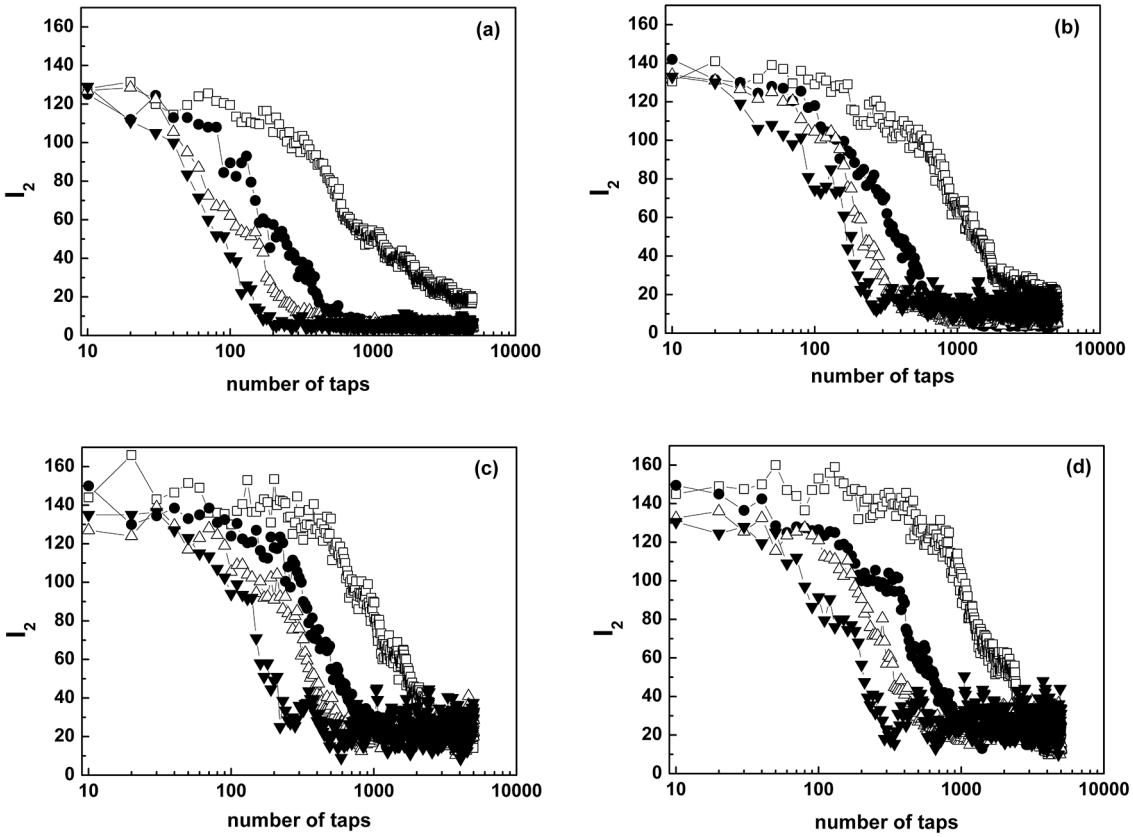

Fig. 9. Segregation index I_2 *vs.* tapping number. (a) $P_0 = 0.00$, (b) $P_0 = 0.01$, (c) $P_0 = 0.10$, (d) $P_0 = 0.25$. In all plots, A is represented by squares, 1.1; solid circles, 1.3; up triangles, 1.5; and solid down triangles, 2.0.

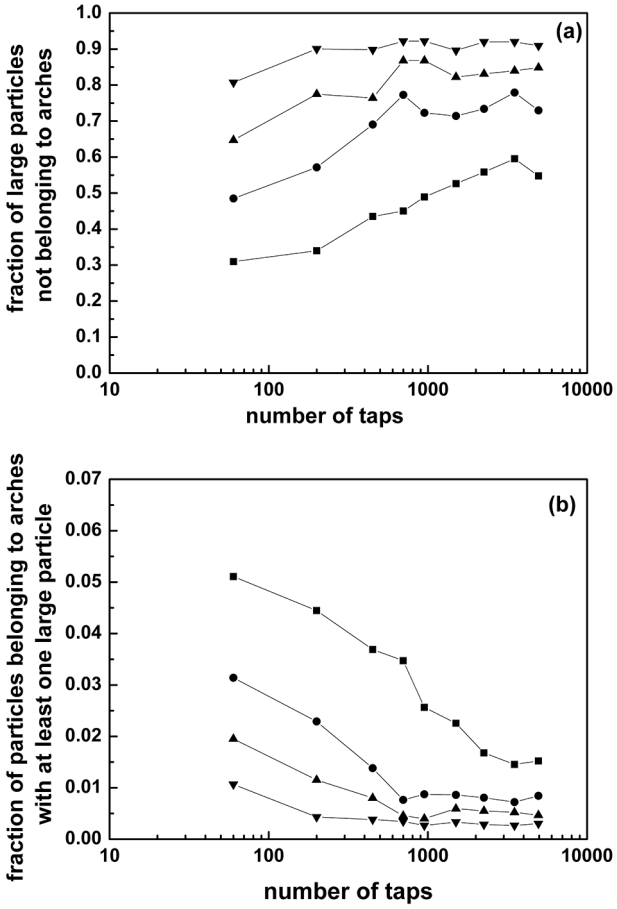

Fig. 10. (a) Fraction number of large particles not belonging to arches *vs.* tapping number. (b) Fraction number of all particles belonging to arches with at least one large particle *vs.* tapping number. In both plots $R/r = 3.0$, $P_0 = 0.01$ and A is represented by squares, 1.1; circles, 1.3; up triangles, 1.5; and down triangles, 2.0.

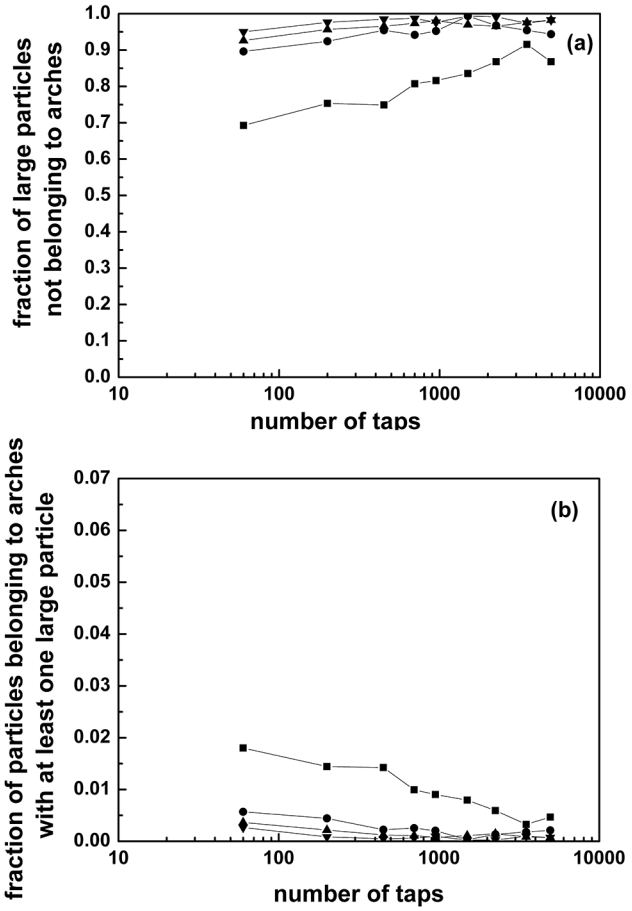

Fig. 11. (a) Fraction number of large particles not belonging to arches *vs.* tapping number. (b) Fraction number of all particles belonging to arches with at least one large particle *vs.* tapping number. In both plots $R/r = 3.0$, $P_0 = 0.1$ and A is represented by squares, 1.1; circles, 1.3; up triangles, 1.5; and down triangles, 2.0.

i.e., a decay is observed and the average values are smaller for the wet case [15]. For tapping intensities greater than 1.1, the fraction remains almost constant throughout the segregation process, unlike for the dry case. This feature is due to the frustration of arch formation induced by the presence of capillary bridges. Indeed, as we will see later, the presence of a high number of capillary bridges implies a low number of particles participating in arches and, besides, the tapping process decreases the number of those bridges. A column with a given wetting degree will start with a given number of particles in arches and this number is prevented by the presence of capillary bridges. As the tapping proceeds, arches decrease but, at the same time, bridges also do. As a result, the number of particles involved in arches stays practically constant. This is not totally true for the case $A = 1.1$ and $P_0 = 0.01$, where the order induced by tapping seems to be still more important to prevent arch formation than for other intensities.

When measuring the size distribution of arches in the column, a rapid decay is observed as the size of the arches increases and this is maintaining all over the tapping process. Besides, as humidity increases, the size distribution of arches decays even more drastically.

4 Conclusions

It is known that the segregation behavior of granular matter is expected to change when humidity is present. Besides, arching has been proven to have an important role in separating particles of different size. However, the concurrent action of arches and capillary bridges is not commonly underlined. In this work we attempt to bring some light to the understanding of the interplay between these two quantities in the segregation process of a tapped column of disks. It is our intention to show, essentially, a qualitative description for understanding the basic mechanisms of the segregation phenomenon under the presence of humidity and to compare with the dry case. A high number of taps simulation, like the one presented here, is a very time consuming process. It is extremely hard to perform the adequate number of runs for lowering the statistical

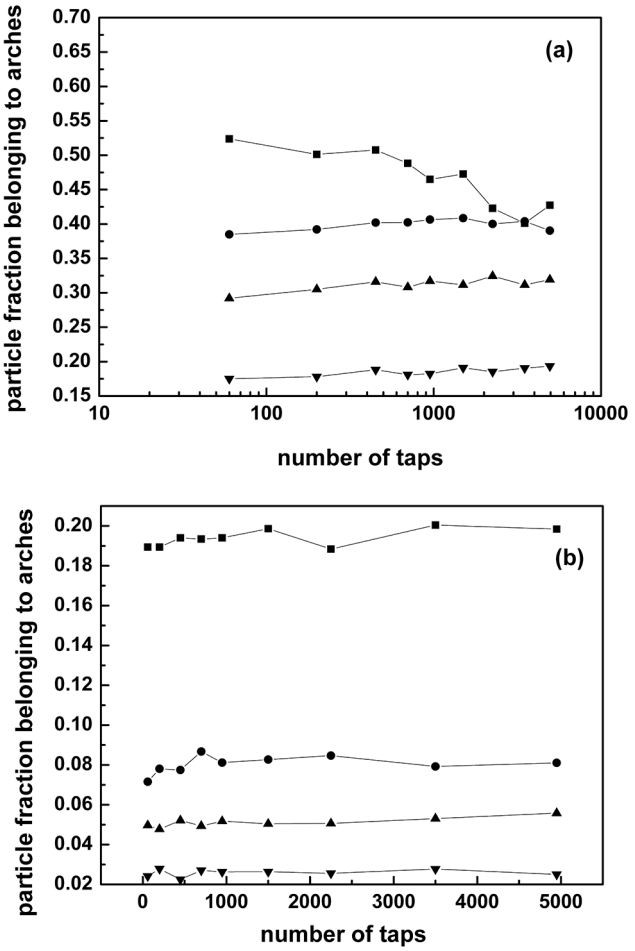

Fig. 12. Fraction number of particles belonging to arches *vs.* tapping number, regardless of the size of the disks and with $R/r = 3.0$. (a) $P_0 = 0.01$ and (b) $P_0 = 0.10$. In both plots, A is represented by squares, 1.1; circles, 1.3; up triangles, 1.5; and down triangles, 2.0.

errors, and this will not necessarily provide a new insight into the problem.

As for the case of an intruder in a dry granular column, we found a critical size ratio (which is expected to depend on the tap amplitude [15]) below which the big particle does not rise for the case of low humidity. This critical threshold is lower for wet columns than for dry ones. For high humidity, the rising velocity is close to zero only for a very low size ratio, *i.e.*, the presence of a large number of capillary bridges favors the climb of the intruder due of the disorder introduced by those interactions.

Disorder is the key for the segregation of intruders that, in a less wet environment, would not get to the surface because of their low size ratio. This is put into evidence when comparing the number of capillary bridges that support a bigger intruder and a smaller one, both particles at the same low humidity, and the same particles at a higher humidity (fig. 7(c) and (d)).

We prove that not only the disorder introduced by a higher tapping intensity will alter the intruder ability to form arches [15] but also the presence of capillary bridges. Taking into account arches and bridges together is of fundamental importance when determining the critical size ratios for the segregation of an intruder.

For wet mixtures, an increase in the tapping intensity promotes the segregation process in all cases but, the presence of a greater number of capillary bridges delays the separation of particles respect to the dry case, although the final state of segregation for higher humidity mixtures after 5000 taps is more evident, especially at low tapping amplitude (see fig. 8(d) and [16]).

The presence of capillary bridges prevents the formation of arches and the compaction of the packing, thus, as humidity increases, the number of particles forming arches is lower. Nevertheless, the absence of arches is balanced by the bridges, making the structure more open and suitable for the rise of the big particles.

It is important to recall again that we do not consider the effects that lubrication or viscosity may have in the segregation of particles. However, in the context of this simple model, we can say that humidity moderates the segregation process in a mixture, although the final segregation state results in the complete separation of big and small particles, independently of the humidity value. This result is in qualitative agreement with the conclusions found in the experiments performed in [16].

Author contribution statement

ROU and AMV developed the simulations and the production of the results. All authors contributed equally to the discussion of the results and writing of the paper.

This work was supported by CONICET (Argentina) through Grant PIP 353 and by the Secretary of Science and Technology of Universidad Nacional de San Luis, Grant P-3-1-0114. ROU wants to acknowledge to the Institut de Physique de Rennes for the hospitality during the stay where most of the present results were discussed.

References

1. R.L. Brown, J. Inst. Fuel **13**, 15 (1939).
2. J.C. Williams, Powder Technol. **15**, 245 (1976).
3. S.-S. Hsiau, W.-C. Chen, Adv. Powder Technol. **13**, 301 (2002).
4. M. Pica Ciamarra, M.D. De Vizia, A. Fierro, M. Tarzia, A. Coniglio, M. Nicodemi, Phys. Rev. Lett. **96**, 058001 (2006).
5. J.G. Benito, R.O. Uñac, A.M. Vidales, I. Ippolito, Physica A **396**, 19 (2014).
6. P. Meakin, Physica A **163**, 733 (1990).
7. G.F. Salter, R.J. Farnish, M.S.A. Bradley, A.J. Burnett, Proc. Inst. Mech. Eng. E **3**, 197 (2000).
8. T. Shinbrot, A. Alexander, F.J. Muzzio, Nature **397**, 675 (1999).
9. M.J. Metzger, B. Remy, B.J. Glasser, Powder Technol. **205**, 42 (2011).

10. S.C. Yang, Powder Technol. **164**, 65 (2006).
11. M. Majid, P. Walzel, Powder Technol. **192**, 311 (2009).
12. H.M. Jaeger, S.R. Nagel, Science **255**, 1523 (1992).
13. V.N. Dolgunin, A.N. Kudy, A.A. Ukolov, Powder Technol. **96**, 211 (1998).
14. W.R. Ketterhagen, J.S. Curtis, C.R. Wassgren, A. Kong, P.J. Narayan, B.C. Hancock, Chem. Eng. Sci. **62**, 6423 (2007).
15. R.O. Uñac, J.G. Benito, A.M. Vidales, L.A. Pugnaloni, Eur. Phys. J. E **37**, 117 (2014).
16. C.-C. Liao, S.-S Hsiau, T.-H. Tsai, C.-H. Tai, Chem. Eng. Sci. **65**, 1109 (2010).
17. N. Mitarai, F. Nori, Adv. Phys. **55**, 1 (2006) and references therein.
18. S.S. Manna, D.V. Khakhar, Phys. Rev. E **58**, R6935 (1998).
19. S.S. Manna, H.J. Herrmann, Eur. Phys. J. E **1**, 341 (2000).
20. L.A. Pugnaloni, M.G. Valluzi, L.G. Valluzzi, Phys. Rev. E **73**, 051302 (2006).
21. R.O. Uñac, A.M. Vidales, L.A. Pugnaloni, Granular Matter **11**, 371 (2009).
22. R.O. Uñac, A.M. Vidales, Granular Matter **13**, 365 (2011).
23. A. Kudrolli, Rep. Prog. Phys. **67**, 209 (2004).
24. A. Anand, J.S. Curtis, C.R. Wassgren, B.C. Hancock, W.R. Ketterhagen, Chem. Eng. Sci. **64**, 5268 (2009).
25. S.J. Gregg, K.S.W. Sing, *Adsorption, surface area, and porosity*, 2nd edition (Academic Press, London, 1982).
26. S. Herminghaus, Adv. Phys. **54**, 221 (2005).
27. S.C. Yang, S.-S. Hsiau, Chem. Eng. Sci. **56**, 6837 (2001).
28. R. Arévalo, D. Maza, L.A. Pugnaloni, Phys. Rev. E **74**, 021303 (2006).
29. J. Duran, J. Rajchenbach, E. Clément, Phys. Rev. Lett. **70**, 2431 (1993).
30. J. Duran, T. Mazozi, E. Clément, J. Rajchenbach, Phys. Rev. E **50**, 5138 (1994).
31. L.A. Pugnaloni, G.C. Barker, A. Mehta, Adv. Complex Syst. **4**, 289 (2001).
32. L.A. Pugnaloni, G.C. Barker, Physica A **337**, 428 (2004).
33. L.A. Pugnaloni, M. Mizrahi, C.M. Carlevaro, F. Vericat, Phys. Rev. E **78**, 051305 (2008).
34. A. Rosato, K.J. Strandburg, F. Prinz, R.H. Swendsen, Phys. Rev. Lett. **58**, 1038 (1987).
35. G.C. Barker, A. Mehta, Europhys. Lett. **29**, 61 (1995).
36. R. Jullien, P. Meakin, A. Pavlovitch, Europhys. Lett. **22**, 523 (1993).